Available online at www.sciencedirect.com

ScienceDirect

journal homepage: www.elsevier.com/locate/he

Electrodeposition of Ni–Fe micro/nano urchin-like structure as an efficient electrocatalyst for overall water splitting

E. Hatami [a], *A. Toghraei* [a], *Ghasem Barati Darband* [a,b,*]

[a] *Department of Materials Engineering, Faculty of Engineering, Tarbiat Modares University, P.O. Box 14115-143, Tehran, Iran*

[b] *Materials and Metallurgical Engineering Department, Faculty of Engineering, Ferdowsi University of Mashhad, Mashhad, 91775-1111, Iran*

HIGHLIGHTS

- Ni–Fe-urchin-like structure was developed using electrodeposition.
- Ni–Fe nanostructure showed outstanding electrocatalytic activity.
- Synergistic effect and high surface area were the factors contributed in this excellent activity.
- Fabricated nanostructure exhibited favorable catalytic stability.

GRAPHICAL ABSTRACT

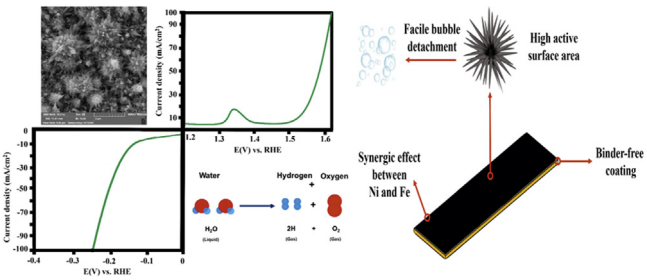

ARTICLE INFO

Article history:
Received 6 September 2020
Received in revised form
15 December 2020
Accepted 16 December 2020
Available online xxx

Keywords:
Electrodeposition
Electrocatalyst
Hydrogen evolution reaction
Urchin-like nanostructure
Oxygen evolution reaction

ABSTRACT

The usage of active electrocatalysts is a useful approach to accelerate the kinetics of electrochemical reactions and to enhance the efficiency of water splitting. To fabricate active electrocatalysts, the creation of new structures that can be easily constructed has always been a research interest. Ni–Fe based alloys are generally known as active OER catalyst. However, in this study, a novel Ni–Fe micro/nano urchin-like structure is reported to be active for both HER and OER. This is the first report of the fabrication of this morphology by a fast, one-step, and affordable electrodeposition method as an efficient HER/OER electrocatalyst. The optimized Ni–Fe coating on Cu substrate demonstrated promising HER activity with low overpotentials of −124 and −243 mV at the current densities of −10 and −100 mA cm^{-2}, respectively. Moreover, the fabricated Ni–Fe urchin-like catalyst is highly active toward OER, requiring overpotentials of only 292 and 374 mV to deliver 10 and 100 mA cm^{-2}. The unique structure of the synthesized coating with an abundant number of micro/nano-scale cones is suggested to play a vital role in the superior

* *Corresponding author*. Department of Materials Engineering, Faculty of Engineering, Tarbiat Modares University, P.O. Box 14115-143, Tehran, Iran.
E-mail addresses: qbdarband@yahoo.com, qasembaratidarband@modares.ac.ir (G. Barati Darband).

https://doi.org/10.1016/j.ijhydene.2020.12.110

HER/OER activity of the catalyst. This article introduces a cost-effective method for the fabrication of a novel urchin-like Ni–Fe alloy as a highly active bifunctional water splitting electrocatalyst.

Introduction

Nowadays, due to the lack of non-renewable energy sources like fossil fuels, it is essential to replace them with sustainable renewable resources. Hydrogen is a promising renewable energy source, which has significant advantages over the others, including remarkable energy density per mass (120–142 MJ/kg) and the zero-emission characteristic [1,2]. One of the main methods of hydrogen production is electrolysis of water, where oxygen evolution reaction (OER) and hydrogen evolution reaction (HER) occur on the anode and cathode surfaces, respectively. However, these reactions are involved in several interactions between the electrode surfaces, ions, and electrons, resulting in the slow kinetics of water splitting [3–5]. To overcome this challenge, the usage of electrocatalysts has been considered as a promising approach that can greatly increase the efficiency of water splitting. Pt-based materials are known as highly active HER electrocatalysts, whereas for OER, the state-of-the-art catalysts are Ir, Ru, and their compositions. Nevertheless, researchers are trying to find adequate alternatives for these costly and rare materials for industrial applications [6,7].

Transition metals are generally recognized as cheap water splitting electrocatalysts with acceptable catalytic activity. Among them, Ni and its alloys have been the focus of researchers regarding their favorable intrinsic electrocatalytic activity [8–12]. Considering various studied nickel alloys such as Ni-Co [13], Ni-Mo [14], and Ni–Fe [15], the last one has attracted the attention of researchers because of its high potential as an active electrocatalyst through both HER and OER. This unique feature enables the Ni–Fe alloy to be used as a bifunctional water splitting electrocatalyst. Using bifunctional catalysts is a fruitful approach to design simple electrolysis systems where both the electrochemical half-reactions occur in a single electrolyte. Discovering such electrocatalysts reduces the costs and provides the opportunity to produce hydrogen and oxygen on a large industrial scale [16]. Although several Ni–Fe based electrocatalysts were studied through HER or OER, only a few of them have been reported to be active for overall water splitting. For instance, although Ni–Fe (oxy) hydroxides have been introduced as highly active through OER, many of them are poor HER catalysts [17]. As a result, to get the advantages of bifunctional electrocatalysts, there is still a need to introduce Ni–Fe alloys that are not only active OER catalysts but also active through HER.

Ni–Fe based electrocatalysts can be synthesized by various techniques such as hydrothermal [18], co-precipitation [19], and solvothermal methods [20]. However, all the mentioned methods are relatively time-consuming, and they need to be done at high temperatures. For instance, Zhong et al. hydrothermally synthesized Ni_2Fe layered double hydroxide (LDH) on carbon paper in an autoclave at 90 °C for 6 h. The required overpotential of the synthesized catalyst at the current density of 10 mA cm^{-2} (η_{10}) was reported to be 289 mV in 1 M KOH solution [21]. In another study, the solvothermal synthesis of NiFe LDH on reduced graphene oxide takes about 20 h at the temperature ranging from 120 °C to 160 °C (η_{10} of OER in 1 M KOH = 245 mV) [22].

Electrodeposition is a facile and fast method to synthesize Ni–Fe based alloys at ambient temperature [14,23,24]. For example, Lu and his co-worker electrodeposited Ni–Fe LDH on the surface of Ni foam in only 300s and measured its OER activity in 1 M KOH, which shows high activity and durability, especially in high current densities [25]. In contrast to many other fabrication procedures, electrodeposition is considered as a binder-free synthesizing method. By eliminating the need for polymeric binders, higher electrical conductivity can be attained, which results in an increase in catalytic activity. Furthermore, the self-supported catalysts usually have higher catalytic durability, especially at high current densities where the produced bubbles can pull off the catalyst loading in the case of using binders [26].

One of the common and effective ways to enhance the electrocatalytic activity is to increase the accessible catalyst active sites by synthesizing nanostructured morphologies. The other advantage of these morphologies is that the produced bubbles can detach from the catalyst surface easily since the nanostructured surface cause a reduction in bubble sizes and bubble adhesion force, as well as modifying the catalyst wettability [27]. The morphology of electrocatalysts is greatly affected by their synthesizing method. Electrodeposition is a fast and cheap method to synthesize various nanostructures. In this approach, it is possible to fabricate a variety of nanostructured morphologies simply by changing the electrodeposition parameters such as the temperature and the electrodeposition bath composition [14]. The most commonly reported nanostructured morphologies of Ni–Fe alloys are nanosheets [16] and nanotubes [28]. However, there are limited studies on certain nanostructures. For instance, to the best of our knowledge, the micro/nano urchin-like morphology has not been reported for Ni–Fe alloys as of yet.

In this study, a facile and one-step electrodeposition method was employed for the first time to synthesize urchin-like Ni–Fe alloy as a bifunctional HER/OER electrocatalyst in alkaline electrolyte. The urchin-like Ni–Fe morphology was synthesized by a one-step galvanostatic method, using $CaCl_2.2H_2O$ as the capping reagent and dissolving different concentrations of Fe^{2+} in the electrodeposition bath [29]. The electrochemical tests in 1 M KOH solution highlight the high activity of Ni–Fe

Please cite this article as: Hatami E et al., Electrodeposition of Ni–Fe micro/nano urchin-like structure as an efficient electrocatalyst for overall water splitting, International Journal of Hydrogen Energy, https://doi.org/10.1016/j.ijhydene.2020.12.110

alloy as a bifunctional HER/OER electrocatalyst. The synthesized catalyst also proved to be stable through the long-term electrolysis at high current densities. The excellent stability and catalytic activity of the synthesized catalyst can be ascribed to its binder-free fabrication method and the synergistic effect of Fe and Ni, which cause a significant increase in the intrinsic activity. Moreover, the urchin-like morphology provides abundant active sites for the electrochemical reactions.

Experimental details

Materials

Iron chloride tetrahydrate ($FeCl_2.4H_2O$), nickel chloride hexahydrate ($NiCl_2.6H_2O$), calcium chloride dihydrate ($CaCl_2 \cdot 2H_2O$), and potassium hydroxide (KOH) were purchased from Merck Co. from analytical grade.

Synthesis of Ni–Fe urchin-like nanostructures

Ni–Fe urchin-like nanostructures were fabricated on the copper substrate by a one-step electrodeposition method. First, Cu sheets (4 cm × 1 cm) were mechanically polished with up to grade 3000 sandpapers, and then they were ultrasonically degreased with acetone for 15 min. Before the electrodeposition step and in order to properly activate the surface, 20% HCl was used. The electrodeposition bath was contained $NiCl_2.6H_2O$ (1 M), $CaCl_2.2H_2O$ (1.2 M), and $FeCl_2.4H_2O$ concentration of 10, 20, 30, 40, and 50 g L^{-1} to evaluate the effect of Fe^{2+} ions on the morphologies of the samples. The temperature was fixed at 60 °C, and the pH of the solution was measured to be about 2.5 for low Fe^{2+} concentrations, which decreased to about 2.4 by increasing the Fe^{2+} content. A Ni sheet was used as the anode, and a steady current density of −40 mA cm^{-2} was applied for 10 min. After the coating process, the samples were washed with distilled water and then left to dry at room temperature.

Structural characterization

Field emission scanning electron microscopy (FE-SEM, TESCAN MIRA3) with a dispersive energy X-ray (EDS) analyzer was used to study the microstructure of coatings. X-ray diffraction (XRD, Philips X'Pert diffractometer) was used to identify the phases of the coatings over a 2θ range of 10–90°.

Electrochemical measurements

Electrochemical tests were performed in 1 M KOH at room temperature using an AUTOLAB 302N potentiostat/galvanostat. The measurements were done using platinum, saturated calomel electrode (SCE), and the fabricated samples as the counter, reference, and working electrodes, respectively. Linear sweep voltammetry (LSV) tests were carried out at a scanning rate of 1 mV s^{-1}, and the recorded data were adjusted by iR correction. All the measured potentials were converted to the reversible hydrogen electrode (RHE). Electrochemical impedance spectroscopy (EIS) tests were done at three various potentials of −100, −200, and −300 mV, at frequencies ranging from 100 kHz to 100 mHz. The catalytic durability of the synthesized samples was assessed by chronopotentiometry (CP) method at the current density of −100 mA cm^{-2} for 10 h. Moreover, the cyclic durability was studied by comparing the LSV plots before and after 1000 cyclic voltammetry (CV) tests via a scanning rate of 100 mV s^{-1}. In order to calculate the electrochemical active surface area (ECSA), double-layer capacitance (C_{dl}) of the samples was obtained first. CV tests were done at scanning rates of 10–100 mV s^{-1} (interval point = 10 mV s^{-1}) in the non-faradic

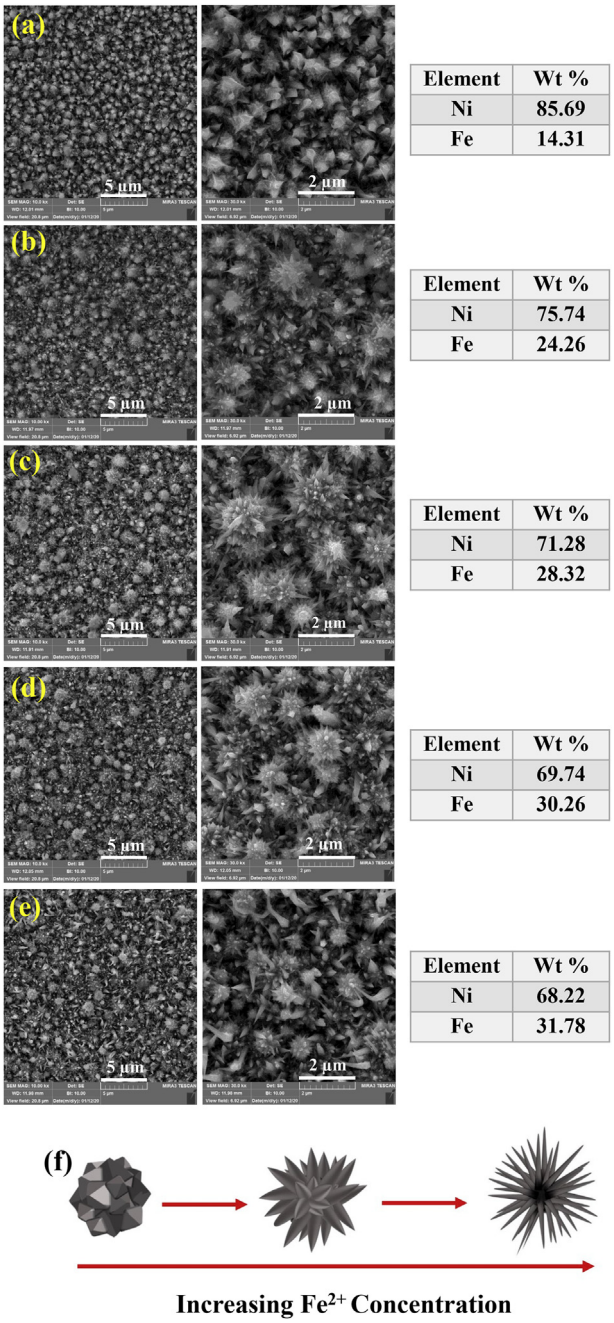

Fig. 1 – EDS results and FESEM images at various magnifications for the Ni–Fe samples synthesized at Fe^{2+} concentrations of (a) 10 g L^{-1}, (b) 20 g L^{-1}, (c) 30 g L^{-1}, (d) 40 g L^{-1}, (e) 50 g L^{-1}. (f) Schematic illustrating the morphology changes by increasing the Fe^{2+} concentration in the electrodeposition bath.

Please cite this article as: Hatami E et al., Electrodeposition of Ni–Fe micro/nano urchin-like structure as an efficient electrocatalyst for overall water splitting, International Journal of Hydrogen Energy, https://doi.org/10.1016/j.ijhydene.2020.12.110

potential range, and the C_{dl} value was calculated using the following formula [30]:

$$C_{dl} = (j_{anodic} - j_{cathodic}) / v$$

In the above formula, j is the current density at the open circuit potential, and v is the CV scan rate.

The ECSA value was obtained by the formula: $ECSA = C_{dl}/C_s$ where C_s is the specific capacitance of a flat surface (40 ηF cm^{-2}).

Results and discussion

Microstructure and composition

The microstructure of Ni–Fe alloys synthesized at different Fe^{2+} content in the bath is depicted in Fig. 1a–e. As shown in Fig. 1a, at a low Fe^{2+} concentration of 10 g L^{-1}, numerous cones can be detected, which are mostly in micro-scale. Nevertheless, as depicted in Fig. 1b–e, by the increase of Fe^{2+} content, urchin-like morphology appears. As schematically shown in Fig. 1f, by increasing Fe^{2+} in the electrodeposition bath, many sharp nanocones grow on the sphere-like structures, which form the urchin-like structure. The mechanism behind the formation of the sharp nanocones can be attributed to the role of Fe^{2+} content in increasing the differences of chemical potential in the solid-liquid interface that reduce the diameter of nanocones [13]. Moreover, $CaCl_2$, as the capping reagent, also contributes to the formation of micro/nano-scale cones. To illustrate, the screw dislocation growth theory should be explained first. According to this theory, the screw dislocations can be the nucleation sites for the growth of nanocones. This growth can occur through the direction of the dislocation core or through its edges. When capping

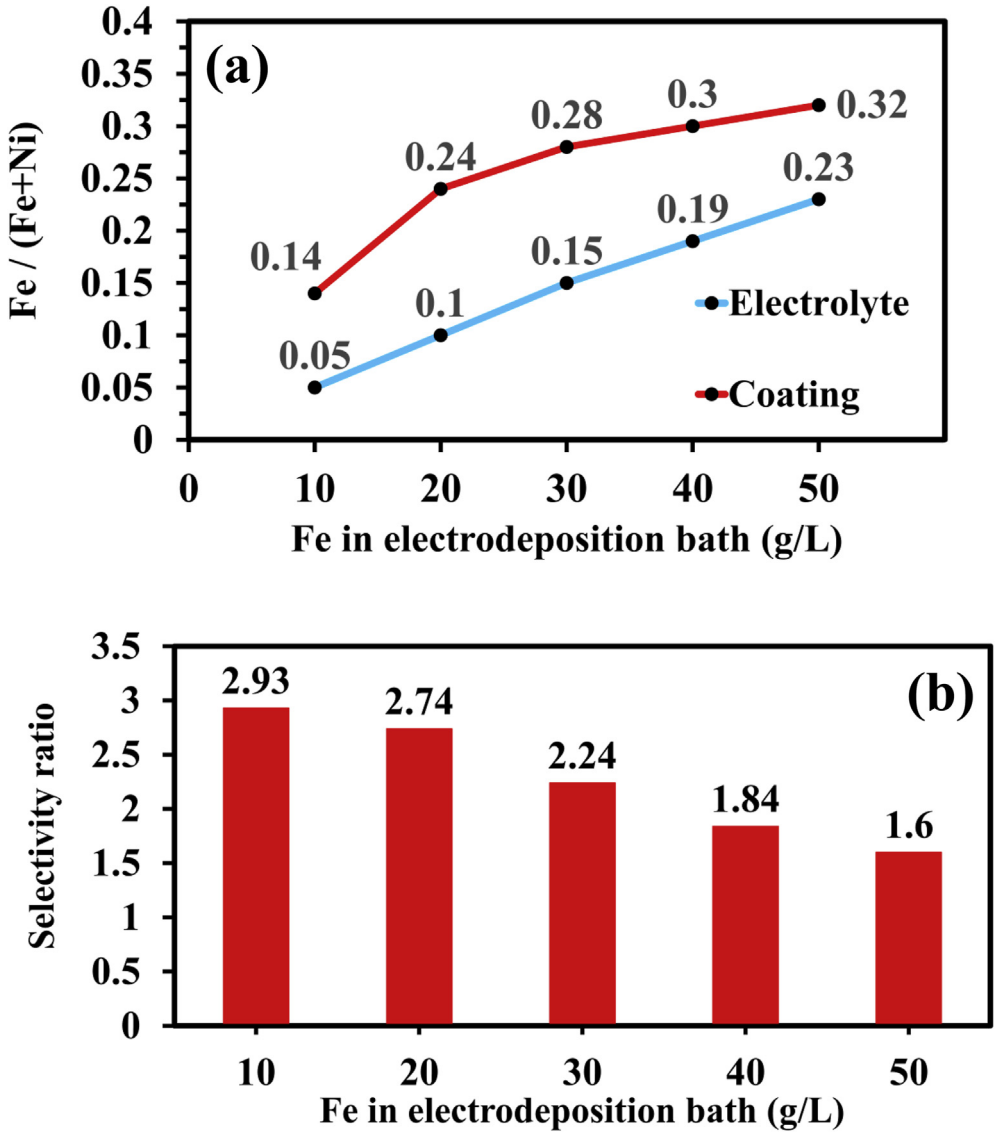

Fig. 2 – (a) Comparison between Fe/(Fe+Ni) value in the electrolyte and coating at different concentration of Fe^{2+} in the electrodeposition bath. (b) Selectivity ratio of the anomalous co-deposition.

Please cite this article as: Hatami E et al., Electrodeposition of Ni–Fe micro/nano urchin-like structure as an efficient electrocatalyst for overall water splitting, International Journal of Hydrogen Energy, https://doi.org/10.1016/j.ijhydene.2020.12.110

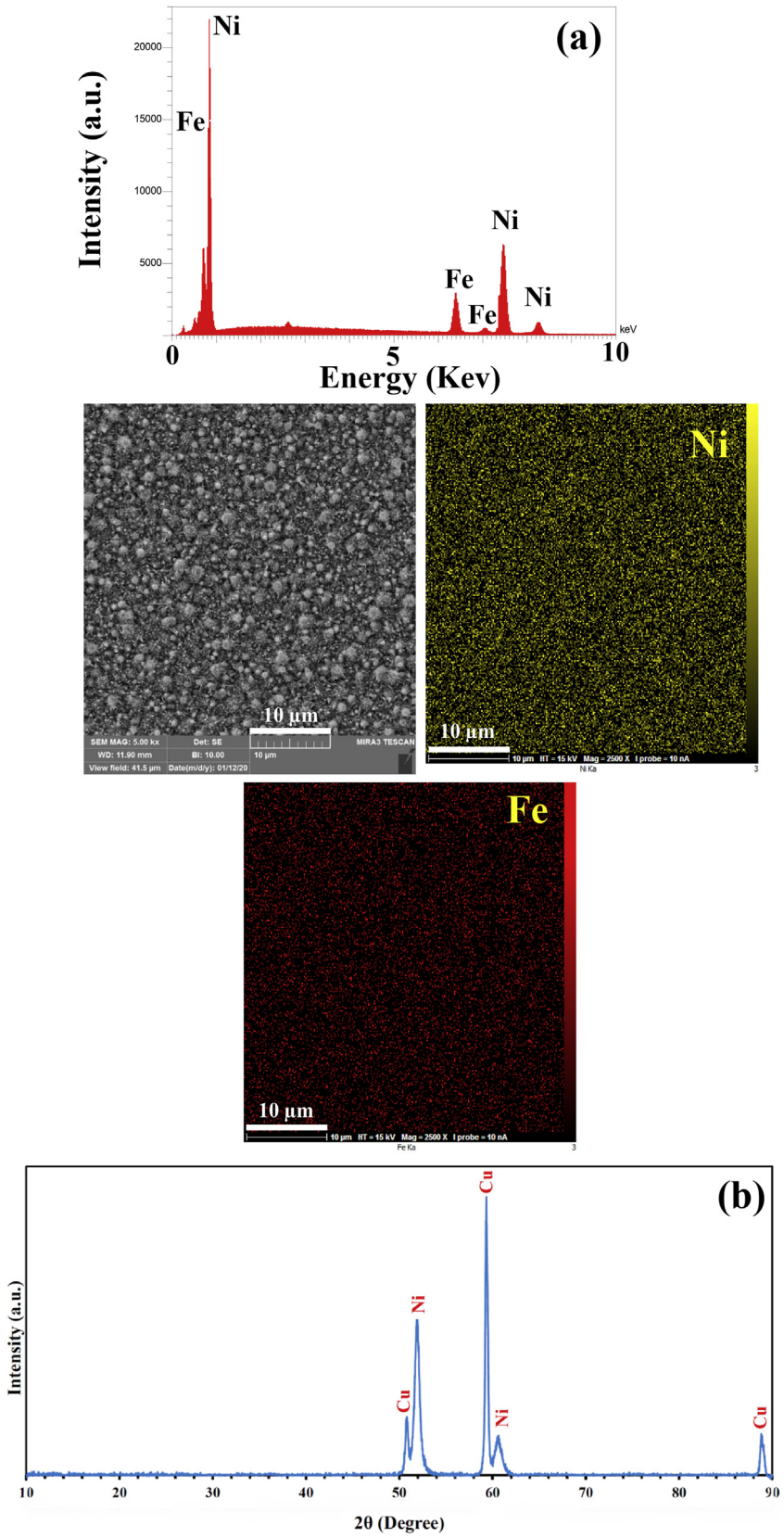

Fig. 3 – (a) EDS results and Elemental EDS mapping of Ni and Fe for the Ni–Fe sample synthesized at 30 g L^{-1} Fe^{2+}. (b) XRD pattern of the Ni–Fe sample synthesized at 30 g L^{-1} Fe^{2+}.

Please cite this article as: Hatami E et al., Electrodeposition of Ni–Fe micro/nano urchin-like structure as an efficient electrocatalyst for overall water splitting, International Journal of Hydrogen Energy, https://doi.org/10.1016/j.ijhydene.2020.12.110

reagents are used, the growth mainly occurs through the direction of dislocation edges, forming sharp nanocones [29,31]. Finally, the tip-discharge phenomena can also play a role in inducing the vertical growth of nanocones [32]. The urchin-like structure not only enhances the ECSA value but also eases the detachment of gas bubbles from the surface of the electrode and improves the electrocatalytic activity [33].

The EDS results for each of the Ni–Fe samples are shown in Fig. 1a–e. Based on these results, and as shown in Fig. 2a, by increasing the amount of Fe^{2+} in the electrodeposition bath, the weight percentage of the iron in the coating was increased. Nevertheless, by comparing the Fe/(Fe+Ni) in the electrodeposition bath and in the coating, an obvious mismatch can be seen. A behavior called "anomalous co-deposition" may be responsible for this observation that Fe/(Fe+Ni) in the coating is higher than the electrolyte. The anomalous co-deposition may take place for the electrodeposition of Fe group alloys, such as Ni, Co, and Fe alloys. In these cases, the deposition of the less noble metal is prior to the nobler one. To study the anomalous co-deposition behavior, a criterion called "selectivity ratio" (SR) has been introduced. SR is known as the atomic ratio of Fe/Ni in a coating to the molar ratio of Fe^{2+}/Ni^{2+} in an electrolyte (Fig. 2b). The SR depends on various factors such as electrolyte characteristics, the coating fabrication method, and the coating thickness [34–36]. Although many studies have been done to study the mechanism of anomalous co-deposition, the exact mechanism has not been fully revealed. According to the Matlosz model [37], the reduction of Ni^{2+} and Fe^{2+} ions takes place in two steps (M stands for Ni or Fe):

$$\text{Step 1: } M(II) + e^- \rightarrow M(I)_{ads} \quad (1)$$

$$\text{Step 2: } M(I)_{ads} + e^- \rightarrow M \quad (2)$$

As can be seen in the above equations, Fe^{2+} and Ni^{2+} ions are firstly reduced by one electron to Fe^{+} and Ni^{+}, and the reduced ions absorb to the surface. In the second step, the reduction rate of Fe^{+} ions is higher than Ni^{+}, so a large proportion of the surface would be covered by Fe^{+} ions, which prohibits the reduction of Ni^{+}. However, other mechanisms are also proposed for the anomalous co-deposition [38,39].

The EDS results and elemental EDS mapping of the Ni–Fe sample synthesized at 30 g L^{-1} Fe^{2+} are depicted in Fig. 3a, in which the homogeneous dispersion of Ni and Fe can be seen on the surface. XRD analysis was done to study the crystallographic phases of the optimized Ni–Fe sample, which was fabricated at a Fe^{2+} concentration of 30 g L^{-1}. As can be seen in Fig. 3b, the peaks of Ni and Cu can be detected in the

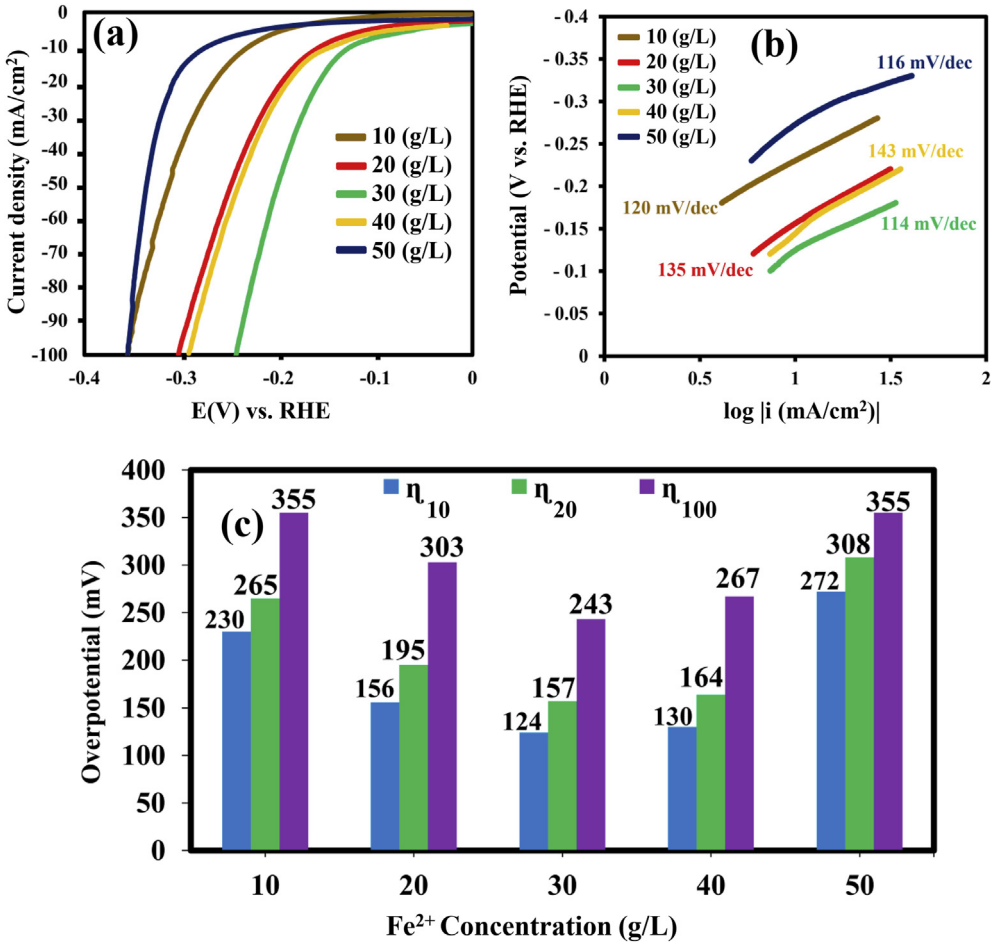

Fig. 4 – HER performance of Ni–Fe samples in 1 M KOH: (a) LSV plots. (b) Tafel plots of different samples. (c) Required overpotentials at −10, −20 and −100 mA cm^{-2} current densities.

Please cite this article as: Hatami E et al., Electrodeposition of Ni–Fe micro/nano urchin-like structure as an efficient electrocatalyst for overall water splitting, International Journal of Hydrogen Energy, https://doi.org/10.1016/j.ijhydene.2020.12.110

XRD spectrum of the Ni–Fe sample. Since the coating thickness is low, the Cu peaks can be attributed to the substrate. The Ni (111) and Ni (200) peaks indicate the FCC crystalline structure. It is noteworthy that no Fe peaks can be detected in the spectrum. This means that Ni and Fe atoms may have formed a solid solution regarding their close atomic radius. This is also in conformity with the Ni–Fe phase diagram [40].

HER electrocatalytic activity and stability

To evaluate and compare the electrocatalytic activity of different materials, certain criteria can be used. One of the most common approaches to do so is to compare the overpotentials at current densities of −10, −20, and −100 mA cm^{-2}, which are shown by η_{10}, η_{20}, and η_{100} symbols, respectively [41]. The LSV tests were done to measure the catalytic activity

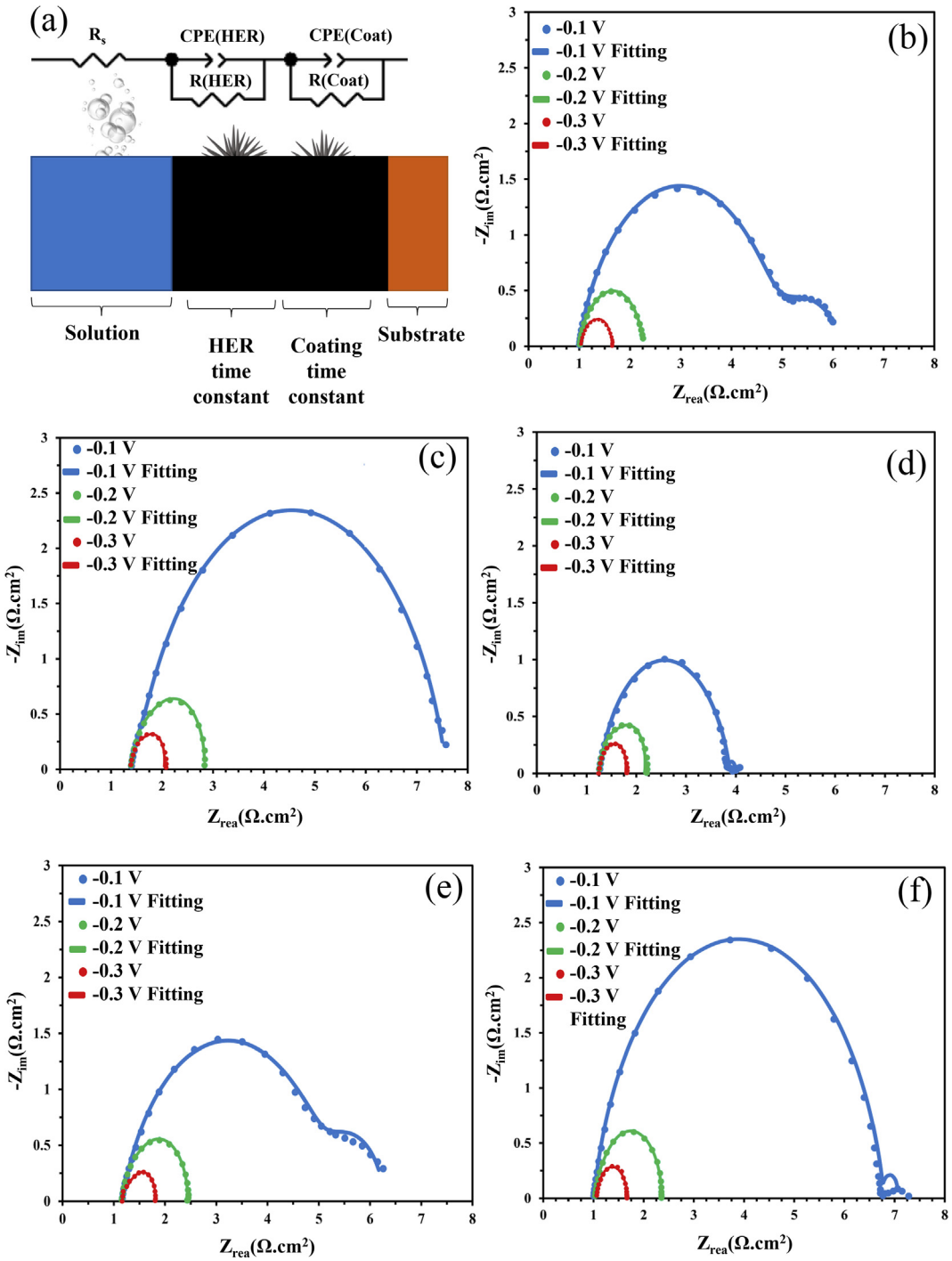

Fig. 5 – (a) Equivalent electrical circuit used for fitting the EIS data, and Nyquist curves at the overpotential of −100, −200 and −300 mV for the Ni–Fe samples synthesized at Fe^{2+} concentrations of (b) 10 g L^{-1}, (c) 20 g L^{-1}, (d) 30 g L^{-1}, (e) 40 g L^{-1}, and (f) 50 g L^{-1}.

Please cite this article as: Hatami E et al., Electrodeposition of Ni–Fe micro/nano urchin-like structure as an efficient electrocatalyst for overall water splitting, International Journal of Hydrogen Energy, https://doi.org/10.1016/j.ijhydene.2020.12.110

of Ni–Fe alloys synthesized at different concentrations of Fe^{2+} in the electrodeposition bath. As shown in Fig. 4a, the sample synthesized at 30 g L^{-1} Fe^{2+} possesses the highest current density at every potential in comparison with the other samples. The η_{10}, η_{20}, and η_{100} values of the optimum Ni–Fe sample were obtained to be −124, −157, and −243 mV, respectively.

To find out the reasons behind the higher HER activity of the sample deposited at 30 g L^{-1} Fe^{2+}, two factors should be considered, which are the intrinsic activity of the catalyst and its morphology. To evaluate the role of intrinsic activity in the HER performance, the LSV curves were normalized to the ECSA value. As can be seen in Fig. S1, the sample deposited at 30 g L^{-1} Fe^{2+} possesses the highest intrinsic HER activity. It has been proposed that the Fe addition to Ni can improve its intrinsic activity by tuning the ad/desorption energy and providing more active sites for the ad/desorption of HER intermediates on the catalyst surface [42,43]. Consequently, it can be concluded that the sample electrodeposited at 30 g L^{-1} Fe^{2+} possesses a high intrinsic activity regarding its optimum amount of Fe content.

However, considering the EDS analysis and the LSV curves, it is noteworthy that although the Fe content of the samples electrodeposited at 30 and 50 g L^{-1} Fe^{2+} are close to each other, the HER activity of the former one is about two times higher than the later. This case highlights the high importance of the catalyst morphology on HER activity. Comparing the C_{dl} value of different Ni–Fe samples (Fig. S2), it can be concluded that the sample deposited at 30 g L^{-1} Fe^{2+} has the highest ECSA value (25 cm^2),which can be attributed to the high number of nanocones in the sample microstructure (Fig. 1c). Rather than the role of the optimum morphology in enhancing the ECSA, the fully-grown urchin-like structure of the optimum sample can decrease the adhesion force of produced O_2 and H_2 bubbles by making the gas-liquid-solid contact line discontinuous [44,45]. This, in turn, can further decrease the required overpotential. Getting benefit from the mentioned features, the HER electrocatalytic activity of the optimized Ni–Fe sample is higher than most of the similar Ni-based catalysts, which were reported in other studies (Table S1).

To evaluate the HER kinetics of the synthesized samples, their Tafel slopes were extracted from the corresponding LSV curves. This can be done by fitting the linear area of LSV plots to the Tafel equation:

$$\eta = a + b\log j \quad (3)$$

In the above formula, a is the intercept, b is the Tafel slope, and j is the current density. Tafel slope is inversely linked to the factor of charge transfer, meaning that the lower the Tafel slope, the charge transfer is faster across the catalyst surface [46]. The Tafel slopes of different Ni–Fe samples are represented in Fig. 4b. The sample synthesized at 30 g L^{-1} Fe^{2+} demonstrates the fastest HER kinetics with the Tafel slope of 114 mV dec^{-1}. Rather than predicting the HER kinetics, the Tafel slope can also be used to indicate the HER mechanism. Three reactions are proposed to be involved in the overall HER process in alkaline electrolyte [47,48]:

Volmer reaction:

$$M + H_2O + e^- \rightarrow OH^- + MH_{ads} \quad (4)$$

Heyrovsky reaction:

$$MH_{ads} + H_2O + e^- \rightarrow M + H_2 + OH^- \quad (5)$$

Tafel reaction:

$$MH_{ads} + MH_{ads} \rightarrow M + H_2 \quad (6)$$

If the Volmer reaction is the rate-determining stage, the Tafel slope is theoretically calculated to be 116 mV dec^{-1} at room temperature (25 °C). This value is obtained to be 39 and 29 mV dec^{-2} in the case of Heyrovsky and Tafel reactions, respectively [41]. Since the Tafel slopes of all the calculated Ni–Fe samples are about 116 mV dec^{-1} or exceed this value (Fig. 4b), Volmer reaction may be the controlling step for the HER process. To have a better comparison of the HER catalytic activity of different Ni–Fe samples, the measured overpotentials at different current densities are represented in Fig. 4c.

To further evaluate the HER kinetics, EIS measurements were conducted at three potentials of −100, −200, and −300

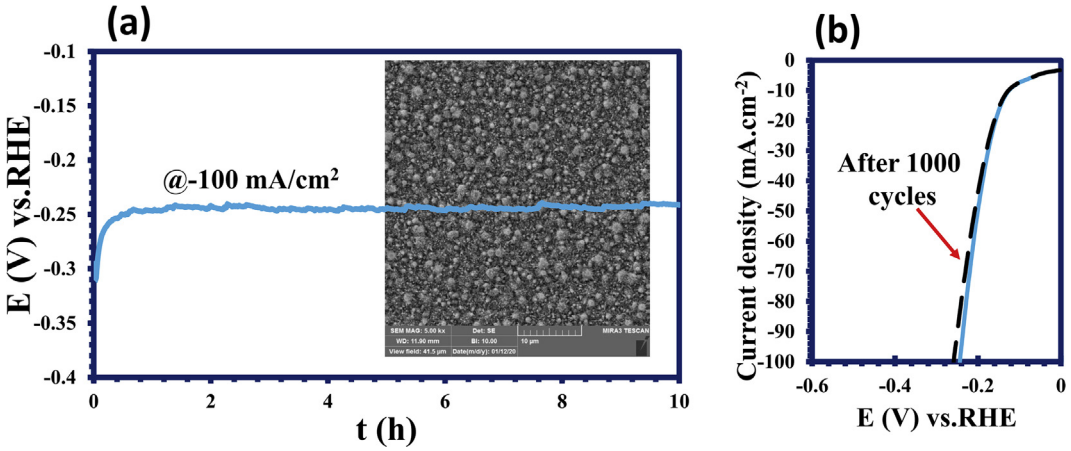

Fig. 6 – (a) Chronopotentiometry curve of Ni–Fe sample synthesized at 30 g L^{-1} Fe^{2+} under current density of −100 mA cm^{-2} during 10 h electrolysis, and the inserted FESEM image of the sample after the 10 h electrolysis (b) LSV curves of Ni–Fe sample synthesized at 30 g L^{-1} Fe^{2+} before and after 1000 voltammetry cycles.

Please cite this article as: Hatami E et al., Electrodeposition of Ni–Fe micro/nano urchin-like structure as an efficient electrocatalyst for overall water splitting, International Journal of Hydrogen Energy, https://doi.org/10.1016/j.ijhydene.2020.12.110

mV. The Nyquist plots of Ni–Fe samples were fitted by an electrical equivalent circuit (EEC), involved of two-time constants. The EEC was chosen based on the physical characteristics of the catalyst's surface with regard to the Nyquist diagram features. As shown in Fig. 5a, R_s is the electrolyte resistance, and there are a couple of parallel units of capacitance and resistance associated with the HER process and the porous coating. Regarding the Nyquist diagrams in Fig. 5b–f, all the curves consist of two semicircles that are well fitted by the proposed EECs. The two semicircles indicate two-time constants. The first time constant is associated with the porous coating surface, and the second one is attributed to the HER process and its kinetics. The second time constant also indicates the easiness of hydrogen bubble release, which is one of the influential parameters in studying the behavior of electrocatalysts [49,50]. Generally, the diameter of the Nyquist curves exhibits the R_2 value or charge transfer resistance. For all the samples, at more negative potentials, the R_2 value is decreased, which indicates the faster HER kinetics at more negative potentials [26]. Comparing the R_2 values of different samples, the one synthesized at 30 g L^{-1} Fe^{2+} has the lowest R_2 value at each of the potentials, which means the fastest HER kinetics. The low R_2 value of the optimized sample emphasizes the role of the high number of micro/nano-scale cones in facilitating the bubble detachment [49].

Rather than high catalytic activity, catalyst stability is another important feature of electrocatalysts for industrial applications [27]. The catalytic durability of the optimum Ni–Fe sample was evaluated by different methods. As shown in Fig. 6a, a negligible potential increase can be observed in the CP curve for the duration of 10 h at the −100 mA cm^{-2} current density, which indicates the excellent stability of the fabricated electrocatalyst. Moreover, as shown in the FESEM image inserted in Fig. 6a, the urchin-like morphology of the Ni–Fe sample is well preserved after 10 h CP analysis, which demonstrates the morphological stability. Furthermore, by comparing the LSV plots before and after 1000 voltammetry cycles (Fig. 6b), a slight positive shift can be detected, which further verifies the high electrochemical durability. One possible reason for this high stability is the binder-free electrodeposition method used to synthesized the samples. The usage of binders in other fabrication methods was reported to decrease the catalyst stability since the catalyst loading may be detached from the substrate during the long-term electrolysis [26].

OER electrocatalytic activity

To examine if the synthesized urchin-like Ni–Fe alloy can be used as a bifunctional electrocatalyst, the OER activity of the

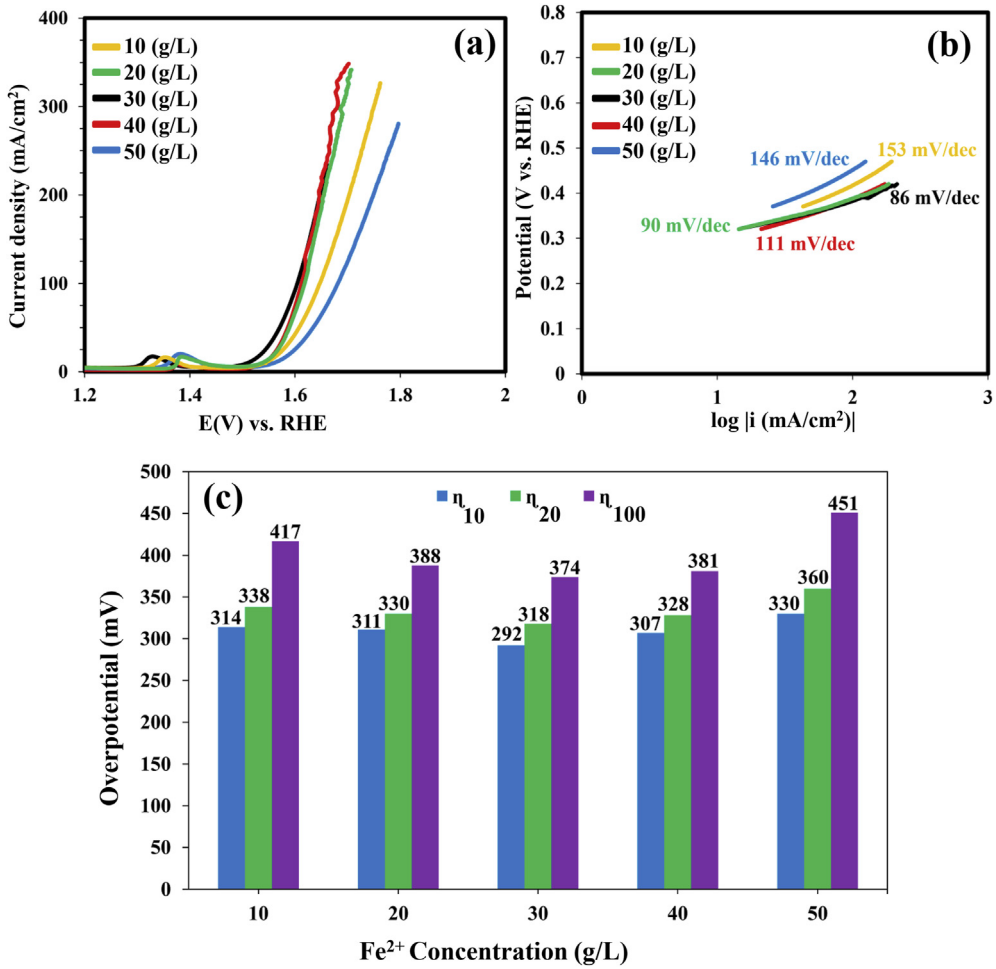

Fig. 7 – OER performance of Ni–Fe samples in 1 M KOH: (a) LSV plots, (b) Tafel plots of different samples. (c) Required overpotentials at 10, 20 and 100 mA cm^{-2} current densities.

Please cite this article as: Hatami E et al., Electrodeposition of Ni–Fe micro/nano urchin-like structure as an efficient electrocatalyst for overall water splitting, International Journal of Hydrogen Energy, https://doi.org/10.1016/j.ijhydene.2020.12.110

samples was studied in the 1 M KOH solution. In comparison with the HER process that consists of two electrons transfer, OER involves in complex intermediate reactions and the exchange of four electrons, resulting in slower kinetics and higher overpotential [51]. Generally, the widely-accepted mechanism for OER in the alkaline electrolyte is proposed as follows [7]:

$$M + OH^- \rightarrow MOH + e^- \quad (7)$$

$$MOH + OH^- \rightarrow MO + H_2O + e^- \quad (8)$$

$$MO + OH^- \rightarrow MOOH + e^- \quad (9)$$

$$MOOH + OH^- \rightarrow H_2O + MO_2 + e^- \quad (10)$$

$$MO_2 \rightarrow M + O_2 \quad (11)$$

To evaluate the OER electrocatalytic activity of the Ni–Fe samples, LSV tests were conducted in 1 M KOH solution. The LSV curves of the samples are depicted in Fig. 7a. Similar to the case of HER, the Ni–Fe sample synthesized at 30 g L^{-1} Fe^{2+} shows the highest OER catalytic activity, as well as the highest intrinsic activity among the other samples (Fig. S3). The overvoltage values of this sample at the 10, 20, and 100 mA cm^{-2} current densities were measured to be 292, 318, and 374 mV, respectively. This result indicates that the well-grown urchin-like morphology of the sample synthesized at 30 g L^{-1} Fe^{2+} is not only responsible for the superior HER activity, but it is also in account for its outstanding OER electrocatalytic performance. Meanwhile, this is in line with the previous works, which argue the positive effect of the Fe on Ni in Ni–Fe alloys towards OER [52–54]. Using density functional theory (DFT), researchers have proposed that there is a synergistic effect between Ni and Fe atoms that can considerably enhance the OER activity. It is suggested that Fe atoms can stabilize the intermediate radical O species whereas Ni atoms take part in accelerating the O–O bonding formation, resulting in an increase in the overall rate of OER [55,56]. Moreover, as shown in Fig. 7b, the Tafel slope of the sample fabricated at 30 g L^{-1} Fe^{2+} is measured to be 86 mV dec^{-1}, which is lower than the other samples, indicating the fastest OER kinetics. The overpotentials of various Ni–Fe samples at different current densities are represented in Fig. 7c. The optimal urchin-like Ni–Fe sample also shows higher OER catalytic activity than many other Ni-based electrocatalysts (Table S2).

Conclusion

Briefly, a unique urchin-like Ni–Fe nanostructure was fabricated using the electrodeposition technique, and the HER/OER electrocatalytic activity of the synthesized samples was evaluated in 1 M KOH solution. The required overpotential of the optimal sample to reach the current density of −10 mA cm^{-2} was obtained to be −124 mV, which is one of the lowest HER overpotential reported for Ni–Fe catalysts. Moreover, the sample shows high OER catalytic activity with η_{10} value of 292 mV, indicating the capability of the synthesized Ni–Fe alloy to be used as a high-performance bifunctional electrocatalyst. Furthermore, the calculated Tafel slope for the optimized Ni–Fe sample was obtained to be −114 mV dec^{-1} toward HER, and 86 mV dec^{-1} in the case of OER. A major reason for this excellent catalytic activity can be ascribed to the unique morphology of the catalyst. The urchin-like structure of the optimized Ni–Fe sample consists of numerous macro/nano-scale cones that facilitate mass transport, ease the bubble detachment, and provide abundant catalytic sites for both the HER and OER. Moreover, the synergistic effect of Ni and Fe atoms plays an important role in enhancing the intrinsic catalytic activity. The urchin-like Ni–Fe structure fabricated by the facile and affordable electrodeposition method can be a great candidate for large-scale water electrolyzing.

Declaration of competing interest

The authors declare that they have no known competing financial interests or personal relationships that could have appeared to influence the work reported in this paper.

Appendix A. Supplementary data

Supplementary data to this article can be found online at https://doi.org/10.1016/j.ijhydene.2020.12.110.

REFERENCES

[1] Gray HB. Powering the planet with solar fuel. Nat Chem 2009;1:112.
[2] Walter MG, Warren EL, McKone JR, Boettcher SW, Mi Q, Santori EA, et al. Solar water splitting cells. Chem Rev 2010;110:6446–73.
[3] Feng L-L, Yu G, Wu Y, Li G-D, Li H, Sun Y, et al. High-index faceted Ni3S2 nanosheet arrays as highly active and ultrastable electrocatalysts for water splitting. J Am Chem Soc 2015;137:14023–6.
[4] Suntivich J, May KJ, Gasteiger HA, Goodenough JB, Shao-Horn Y. A perovskite oxide optimized for oxygen evolution catalysis from molecular orbital principles. Science 2011;334:1383–5.
[5] Zeng K, Zhang D. Recent progress in alkaline water electrolysis for hydrogen production and applications. Prog Energy Combust Sci 2010;36:307–26.
[6] Lee Y, Suntivich J, May KJ, Perry EE, Shao-Horn Y. Synthesis and activities of rutile IrO2 and RuO2 nanoparticles for oxygen evolution in acid and alkaline solutions. J Phys Chem Lett 2012;3:399–404.
[7] Suen N-T, Hung S-F, Quan Q, Zhang N, Xu Y-J, Chen HM. Electrocatalysis for the oxygen evolution reaction: recent development and future perspectives. Chem Soc Rev 2017;46:337–65.
[8] Darband GB, Aliofkhazraei M, Rouhaghdam AS. Facile electrodeposition of ternary Ni-Fe-Co alloy nanostructure as a binder free, cost-effective and durable electrocatalyst for high-performance overall water splitting. J Colloid Interface Sci 2019;547:407–20.
[9] Li H, Wen P, Li Q, Dun C, Xing J, Lu C, et al. Earth-abundant iron diboride (FeB2) nanoparticles as highly active

bifunctional electrocatalysts for overall water splitting. Adv Energy Mater 2017;7:1700513.
[10] Zhang L, Liu B, Zhang N, Ma M. Electrosynthesis of Co 3 O 4 and Co (OH) 2 ultrathin nanosheet arrays for efficient electrocatalytic water splitting in alkaline and neutral media. Nano Res 2018;11:323–33.
[11] Lu S-S, Zhang L-M, Dong Y-W, Zhang J-Q, Yan X-T, Sun D-F, et al. Tungsten-doped Ni–Co phosphides with multiple catalytic sites as efficient electrocatalysts for overall water splitting. J Mater Chem A 2019;7:16859–66.
[12] Zhang X-Y, Guo B-Y, Chen Q-W, Dong B, Zhang J-Q, Qin J-F, et al. Ultrafine and highly-dispersed bimetal Ni2P/Co2P encapsulated by hollow N-doped carbon nanospheres for efficient hydrogen evolution. Int J Hydrogen Energy 2019;44:14908–17.
[13] Darband GB, Aliofkhazraei M, Rouhaghdam AS, Kiani M. Three-dimensional Ni-Co alloy hierarchical nanostructure as efficient non-noble-metal electrocatalyst for hydrogen evolution reaction. Appl Surf Sci 2019;465:846–62.
[14] Toghraei A, Shahrabi T, Darband GB. Electrodeposition of self-supported Ni-Mo-P film on Ni foam as an affordable and high-performance electrocatalyst toward hydrogen evolution reaction. Electrochim Acta 2020;335:135643.
[15] Zhang Y, Xia X, Cao X, Zhang B, Tiep NH, He H, et al. Ultrafine metal nanoparticles/N-doped porous carbon hybrids coated on carbon fibers as flexible and binder-free water splitting catalysts. Adv Energy Mater 2017;7:1700220.
[16] Jia Y, Zhang L, Gao G, Chen H, Wang B, Zhou J, et al. A heterostructure coupling of exfoliated Ni–Fe hydroxide nanosheet and defective graphene as a bifunctional electrocatalyst for overall water splitting. Adv Mater 2017;29:1700017.
[17] Luo J, Im J-H, Mayer MT, Schreier M, Nazeeruddin MK, Park N-G, et al. Water photolysis at 12.3% efficiency via perovskite photovoltaics and Earth-abundant catalysts. Science 2014;345:1593–6.
[18] Dinh KN, Zheng P, Dai Z, Zhang Y, Dangol R, Zheng Y, et al. Ultrathin porous NiFeV ternary layer hydroxide nanosheets as a highly efficient bifunctional electrocatalyst for overall water splitting. Small 2018;14:1703257.
[19] Xing C, Zhang Y, Yan W, Guo L. Band structure-controlled solid solution of Cd1-x ZnxS photocatalyst for hydrogen production by water splitting. Int J Hydrogen Energy 2006;31:2018–24.
[20] Sun T, Liu E, Liang X, Hu X, Fan J. Enhanced hydrogen evolution from water splitting using Fe-Ni codoped and Ag deposited anatase TiO2 synthesized by solvothermal method. Appl Surf Sci 2015;347:696–705.
[21] Zhong H, Cheng X, Xu H, Li L, Li D, Tang P, et al. Carbon fiber paper supported interlayer space enlarged Ni2Fe-LDHs improved OER electrocatalytic activity. Electrochim Acta 2017;258:554–60.
[22] Youn DH, Park YB, Kim JY, Magesh G, Jang YJ, Lee JS. One-pot synthesis of NiFe layered double hydroxide/reduced graphene oxide composite as an efficient electrocatalyst for electrochemical and photoelectrochemical water oxidation. J Power Sources 2015;294:437–43.
[23] Li Z, Shao M, An H, Wang Z, Xu S, Wei M, et al. Fast electrosynthesis of Fe-containing layered double hydroxide arrays toward highly efficient electrocatalytic oxidation reactions. Chem Sci 2015;6:6624–31.
[24] Ganesan P, Sivanantham A, Shanmugam S. Inexpensive electrochemical synthesis of nickel iron sulphides on nickel foam: super active and ultra-durable electrocatalysts for alkaline electrolyte membrane water electrolysis. J Mater Chem A 2016;4:16394–402.
[25] Lu X, Zhao C. Electrodeposition of hierarchically structured three-dimensional nickel–iron electrodes for efficient oxygen evolution at high current densities. Nat Commun 2015;6:1–7.
[26] Darband GB, Aliofkhazraei M, Rouhaghdam AS. Nickel nanocones as efficient and stable catalyst for electrochemical hydrogen evolution reaction. Int J Hydrogen Energy 2017;42:14560–5.
[27] Jamesh MI, Kuang Y, Sun X. Constructing earth-abundant 3D nanoarrays for efficient overall water splitting–A review. ChemCatChem 2019;11:1550–75.
[28] Gong M, Li Y, Wang H, Liang Y, Wu JZ, Zhou J, et al. An advanced Ni–Fe layered double hydroxide electrocatalyst for water oxidation. J Am Chem Soc 2013;135:8452–5.
[29] Lee JM, Jung KK, Lee SH, Ko JS. One-step fabrication of nickel nanocones by electrodeposition using CaCl2· 2H2O as capping reagent. Appl Surf Sci 2016;369:163–9.
[30] Feng Z, Li D, Wang L, Sun Q, Lu P, Xing P, et al. In situ grown nanosheet NiZn alloy on Ni foam for high performance hydrazine electrooxidation. Electrochim Acta 2019;304:275–81.
[31] Jin S, Bierman MJ, Morin SA. A new twist on nanowire formation: screw-dislocation-driven growth of nanowires and nanotubes. J Phys Chem Lett 2010;1:1472–80.
[32] Hang T, Li M, Fei Q, Mao D. Characterization of nickel nanocones routed by electrodeposition without any template. Nanotechnology 2007;19:035201.
[33] You B, Jiang N, Sheng M, Bhushan MW, Sun Y. Hierarchically porous urchin-like Ni2P superstructures supported on nickel foam as efficient bifunctional electrocatalysts for overall water splitting. ACS Catal 2016;6:714–21.
[34] Dragos O, Chiriac H, Lupu N, Grigoras M, Tabakovic I. Anomalous codeposition of fcc NiFe nanowires with 5–55% Fe and their morphology, crystal structure and magnetic properties. J Electrochem Soc 2015;163:D83.
[35] Zech N, Podlaha E, Landolt D. Anomalous codeposition of iron group metals: I. Experimental results. J Electrochem Soc 1999;146:2886.
[36] Brenner A. Electrodeposition of alloys: principles and practice. Elsevier; 2013.
[37] Matlosz M. Competitive adsorption effects in the electrodeposition of iron-nickel alloys. J Electrochem Soc 1993;140:2272.
[38] Hessami S, Tobias CW. A mathematical model for anomalous codeposition of nickel-iron on a rotating disk electrode. J Electrochem Soc 1989;136:3611.
[39] Grande WC, Talbot JB. Electrodeposition of thin films of nickel-iron: II. Modeling. J Electrochem Soc 1993;140:675.
[40] Swartzendruber L, Itkin V, Alcock C. The Fe-Ni (iron-nickel) system. J Phase Equil 1991;12:288–312.
[41] Zhu J, Hu L, Zhao P, Lee LYS, Wong K-Y. Recent advances in electrocatalytic hydrogen evolution using nanoparticles. Chem Rev 2019;120:851–918.
[42] Gong M, Dai H. A mini review of NiFe-based materials as highly active oxygen evolution reaction electrocatalysts. Nano Res 2015;8:23–39.
[43] Long X, Li G, Wang Z, Zhu H, Zhang T, Xiao S, et al. Metallic iron–nickel sulfide ultrathin nanosheets as a highly active electrocatalyst for hydrogen evolution reaction in acidic media. J Am Chem Soc 2015;137:11900–3.
[44] Feng Z, Zhang H, Gao B, Lu P, Li D, Xing P. Ni–Zn nanosheet anchored on rGO as bifunctional electrocatalyst for efficient alkaline water-to-hydrogen conversion via hydrazine electrolysis. Int J Hydrogen Energy 2020 Jul 31;45(38):19335–43.
[45] Feng Z, Li D, Wang L, Sun Q, Lu P, Xing P, et al. A 3D porous Ni-Zn/RGO catalyst with superaerophobic surface for high-performance hydrazine electrooxidation. J Alloys Compd 2019;788:1240–5.

Please cite this article as: Hatami E et al., Electrodeposition of Ni–Fe micro/nano urchin-like structure as an efficient electrocatalyst for overall water splitting, International Journal of Hydrogen Energy, https://doi.org/10.1016/j.ijhydene.2020.12.110

[46] Yan Y, Xia BY, Zhao B, Wang X. A review on noble-metal-free bifunctional heterogeneous catalysts for overall electrochemical water splitting. J Mater Chem A 2016;4:17587–603.
[47] Darband GB, Aliofkhazraei M, Shanmugam S. Recent advances in methods and technologies for enhancing bubble detachment during electrochemical water splitting. Renew Sustain Energy Rev 2019;114:109300.
[48] Eliaz N, Gileadi E. Physical electrochemistry: fundamentals, techniques, and applications. John Wiley & Sons; 2019.
[49] Darband GB, Aliofkhazraei M, Rouhaghdam AS. Three-dimensional porous Ni-CNT composite nanocones as high performance electrocatalysts for hydrogen evolution reaction. J Electroanal Chem 2018;829:194–207.
[50] Fricoteaux P, Rousse C. Influence of substrate, pH and magnetic field onto composition and current efficiency of electrodeposited Ni–Fe alloys. J Electroanal Chem 2008;612:9–14.
[51] Feng Z, Wang E, Huang S, Liu J. A bifunctional nanoporous Ni–Co–Se electrocatalyst with a superaerophobic surface for water and hydrazine oxidation. Nanoscale 2020;12:4426–34.
[52] Liang Y, Liu Q, Asiri AM, Sun X, He Y. Nickel–iron foam as a three-dimensional robust oxygen evolution electrode with high activity. Int J Hydrogen Energy 2015;40:13258–63.
[53] Cheng N, Liu Q, Asiri AM, Xing W, Sun X. A Fe-doped Ni 3 S 2 particle film as a high-efficiency robust oxygen evolution electrode with very high current density. J Mater Chem A 2015;3:23207–12.
[54] Zhang B, Xiao C, Xie S, Liang J, Chen X, Tang Y. Iron–nickel nitride nanostructures in situ grown on surface-redox-etching nickel foam: efficient and ultrasustainable electrocatalysts for overall water splitting. Chem Mater 2016;28:6934–41.
[55] Anantharaj S, Kundu S, Noda S. "The Fe effect": a review unveiling the critical roles of Fe in enhancing OER activity of Ni and Co based catalysts. Nano Energy 2020:105514.
[56] Xiao H, Shin H, Goddard WA. Synergy between Fe and Ni in the optimal performance of (Ni, Fe) OOH catalysts for the oxygen evolution reaction. Proc Natl Acad Sci 2018;115:5872–7.

Please cite this article as: Hatami E et al., Electrodeposition of Ni–Fe micro/nano urchin-like structure as an efficient electrocatalyst for overall water splitting, International Journal of Hydrogen Energy, https://doi.org/10.1016/j.ijhydene.2020.12.110